RECENT ADVANCES IN THE STUDY OF HYDROGEN EMBRITTLEMENT AT THE UNIVERSITY OF ILLINOIS

P. Sofronis[1*], I. M. Robertson[2], Y. Liang[1], D. F. Teter[3], and N. Aravas[4]

University of Illinois at Urbana-Champaign
Frederick Seitz Materials Research Laboratory
Urbana, IL, USA

[1]Department of Theoretical and Applied Mechanics
216 Talbot Laboratory
104 South Wright Street, Urbana, IL 61801, USA

[2]Department of Materials Science and Engineering
1304 West Green Street, Urbana, IL 61801, USA

[3]Materials Science and Technology: Metallurgy (MST-6)
Los Alamos National Laboratory
Mail Stop: G770, Los Alamos, NM 87545, USA

[4]Department of Mechanical and Industrial Engineering
University of Thessaly,
Pedion Areos, 38334 Volos, Greece

September 2001

[*] Corresponding author, email: sofronis@uiuc.edu, FAX #: 217-244 0757

Abstract

This paper summarizes recent work at the University of Illinois on the fundamental mechanisms of hydrogen embrittlement. Our approach combines experimental and theoretical methods. We describe the theoretical work on hydride formation and its application to hydrogen embrittlement of Ti alloys through the stress-induced hydride formation and cleavage mechanism, the localization of shear due to solute hydrogen, and finally, we present experimental evidence that favors the decohesion mechanism of hydrogen embrittlement in a β-Ti alloy.

Preface

It is with the greatest pleasure and honor that we dedicate this paper to our friend and colleague Professor Howard K. Birnbaum of the University of Illinois at Urbana-Champaign, who, in our opinion, has made major contributions to our understanding of the behavior of hydrogen in metals, and to the field of hydrogen embrittlement in general. During our careers he has been an excellent role model with exceptionally high scientific and ethical standards, and he has had a profound effect on our research and teaching. Without Howard's help, encouragement, guidance, and friendship the work presented in this paper would not have been possible.

Introduction

Our previous experimental and modeling work has focused on establishing the influence of hydrogen on the mobility of dislocations throughout a metal; see review papers (1, 2) and references therein for details. In our studies solute hydrogen enhanced the mobility of all dislocation types (edge, screw, and mixed perfect, and partial dislocations) and occurred in a wide range of metals and alloys with different crystal structures. The generality of the effect has been explained in terms of the hydrogen-shielding model in which the presence of hydrogen atmospheres around dislocations and elastic obstacles decreases the interaction energy between them (3). This effect manifests itself as a reduction in the applied stress required to move dislocations in the presence of solute hydrogen and causes highly localized deformation (4-9), which in turn results in highly localized failure by plastic processes. (It is important to appreciate that this dislocation enhancement mechanism by solute hydrogen is fundamentally different from the one proposed by Lynch (10, 11), which is restricted to hydrogen enhancing the injection of dislocations from the surface.) In this paper we summarize more recent work on the stress-induced hydride formation and cleavage mechanism, the localization of plasticity due to solute hydrogen, and hydrogen-induced decohesion.

Hydride Formation and Cleavage

The stress-induced hydride formation and cleavage mechanism is one of the well-established hydrogen embrittlement mechanisms with extensive experimental and theoretical support (12, 13). The nucleation and growth of an extensive hydride field ahead of a crack has been observed dynamically in α-Ti (14) charged from the gas phase *in situ* in a controlled environment transmission electron microscope (15). The hydrides first nucleated in the stress-field of the crack and grew to large sizes not by the growth of individual hydrides but by the nucleation and growth of new hydrides in the stress field of the others. These small hydrides grew together to form the larger hydrides. This autocatalytic process of hydride nucleation and growth can be seen in the images in Figs. 1a and 1b. These images were captured from videotape and show two hydrides, which are outlined for purposes of clarity. Hydride 2 nucleated in the stress field of hydride 1 and the overall growth direction of the hydride is as indicated. This nucleation and growth process continued as long as the hydrogen supply was continually replenished. Associated with the formation of the hydrides is a volume expansion, which can be as large as 30%. The accommodation mechanisms are seen in the images. The change in contrast adjacent to the hydrides is evidence of elastic accommodation. Plastic accommodation also occurs as evidenced by the emission of dislocations from the front of the growing hydride, Fig 1c. For this sample orientation the dislocations emanating from the hydride appear as simple black-white lobes as their line direction is parallel to that of the electron beam. The extensive hydride field that developed ahead of the crack is shown in Fig. 1d. To successfully calculate and simulate the development of the hydride field it is therefore essential that elastic-plastic accommodation effects be taken into account.

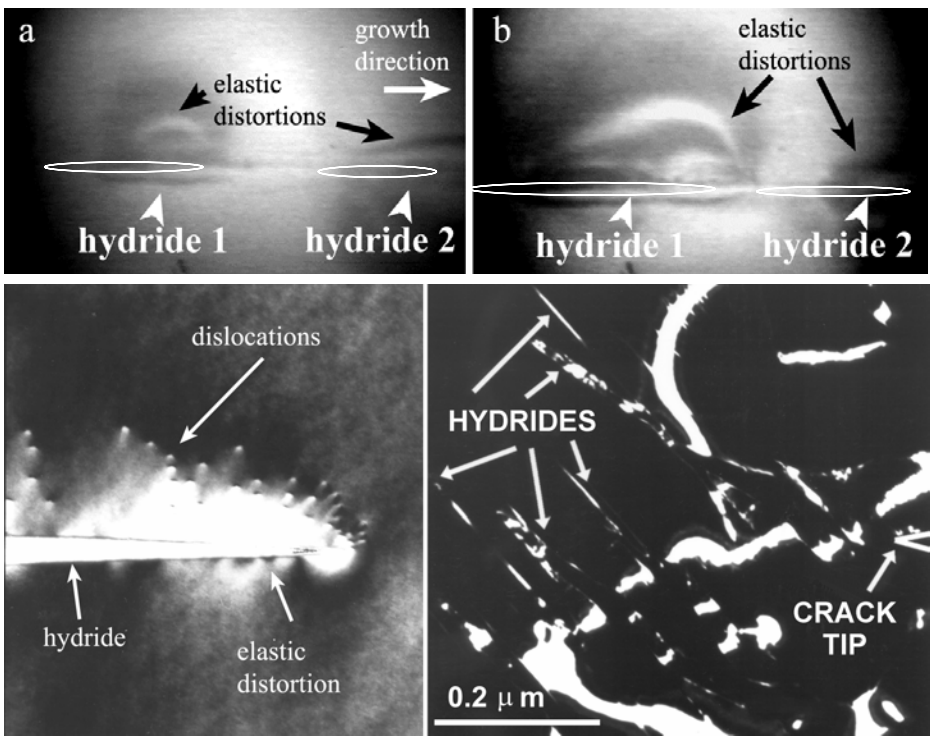

Figure 1: Nucleation and growth of hydrides (a and b). Dislocation emission from a growing hydride (c). Hydride field ahead of a crack (d). Material is α-Ti (14).

Hydride formation under an externally applied stress in a matrix deforming only elastically is characterized by the terminal solid solubility (TSS) (the local solvus concentration) c_s^{σ}, measured in hydrogen atoms per solute atom, and is given by

$$c_s^{\sigma} = B\exp\left(\Delta G^{\text{tot}}_{\alpha-\beta} \middle/ RT\right). \tag{1}$$

In Eqn. (1), B is an experimentally determined constant and $\Delta G^{\text{tot}}_{\alpha-\beta}$ is the total Gibbs free energy change in forming a mole of hydride phase β from the solid solution phase α. Under an externally applied stress $\Delta G^{\text{tot}}_{\alpha-\beta}$ is given by

$$\Delta G^{\text{tot}}_{\alpha-\beta} = \Delta G^{\text{chem}}_{\alpha-\beta} + \Delta G^{\text{sur}}_{\alpha-\beta} + \Delta G^{\text{acc}}_{\alpha-\beta} + \Delta G^{\text{int}}_{\alpha-\beta}, \tag{2}$$

where $\Delta G^{\text{chem}}_{\alpha-\beta}$ is the chemical Gibbs energy change associated with hydride formation, $\Delta G^{\text{sur}}_{\alpha-\beta}$ is the free energy needed for the creation of the interface, $\Delta G^{\text{acc}}_{\alpha-\beta} = W_{\text{acc}}$ is the accommodation energy and $\Delta G^{\text{int}}_{\alpha-\beta} = W_{\text{int}}$ is the elastic interaction energy. As shown in Fig. 1, the assumption of purely elastic accommodation is not strictly applicable as the hydride volume expansion is accommodated both elastically and plastically. Previous attempts to include plasticity effects neglected the externally applied stress and, incorrectly, assumed that the interaction between the externally applied stress and the hydride expansion could, as it can in the elastic solution, be simply superimposed on the accommodation term.

To address this problem, Lufrano et al. (16) have modeled the constitutive material behavior as isotropically linear in the elastic regime and by the Prandtl-Reuss equations in the plasticity regime. The total Gibbs free energy of hydride formation under an externally applied stress for an elastoplastic system can be written as

$$\Delta G^{\text{tot}}_{\alpha-\beta} = \Delta G^{\text{chem}}_{\alpha-\beta} + \Delta G^{\text{sur}}_{\alpha-\beta} + \Delta G^{\text{mech}}_{\alpha-\beta}\ , \tag{3}$$

where $\Delta G^{\text{mech}}_{\alpha-\beta}$ is the total mechanical free energy of hydride formation and $\Delta G^{\text{mech}}_{\alpha-\beta}$ is given by

$$\Delta G^{\text{mech}}_{\alpha-\beta} = \Delta G^{\text{e}}_{\alpha-\beta} + \Delta G^{\text{p}}_{\alpha-\beta} + \Delta G^{\text{ext}}_{\alpha-\beta}. \tag{4}$$

In Eqn. (4) $\Delta G^{\text{e}}_{\alpha-\beta}$ is the elastic work done on the system (matrix+hydride) and is stored in the system as elastic energy, $\Delta G^{\text{p}}_{\alpha-\beta}$ is the plastic work dissipation, and $\Delta G^{\text{ext}}_{\alpha-\beta}$ is the work done by external loads against the matrix displacement upon hydride formation. The change in elastic energy stored in the system, $\Delta G^{\text{e}}_{\alpha-\beta}$, can be evaluated with the use of

$$\Delta G^{\mathrm{e}}_{\alpha-\beta} = \int_V \left(\int_t \sigma_{ij} D^{\mathrm{e}}_{ij} dt \right) dV \,, \tag{5}$$

where σ_{ij} is the local Cauchy stress, D^{e}_{ij} is the elastic component of the deformation rate tensor (which equals the symmetric part of the velocity gradient in spatial coordinates), t is the time of formation, and V is the volume of the system (matrix+hydride). The plastic work done on the system, $\Delta G^{\mathrm{p}}_{\alpha-\beta}$, can be evaluated with the use of

$$\Delta G^{\mathrm{p}}_{\alpha-\beta} = \int_V \left(\int_t \sigma_{ij} D^{\mathrm{p}}_{ij} dt \right) dV \,, \tag{6}$$

where D^{p}_{ij} is the plastic component of the deformation rate tensor. The work done by the external tractions, $\Delta G^{\mathrm{ext}}_{\alpha-\beta}$, can be evaluated with the use of

$$\Delta G^{\mathrm{ext}}_{\alpha-\beta} = \int_S \left(\int_t T^{\mathrm{ext}}_i v_i dt \right) dS \,, \tag{7}$$

where S is the surface bounding the volume V, T^{ext}_i is the component of the applied traction on S, and v_i is the component of the surface velocity. Numerical calculations were carried out to estimate the total mechanical energy of formation of a hydride precipitate with an isotropic linearly elastic response in an infinite niobium matrix with an isotropic linearly elastic, perfectly plastic response under plane strain conditions. In this treatment, it was assumed that the entire volume of the precipitate uniformly acquires the transformation strain that accompanies hydride formation. The results of the calculations can be summarized as follows. For purely elastic accommodation, the solvus concentration of hydrogen in solution is

$$c^{\sigma}_s = 3.74 \exp\left(\frac{-10.6\,\mathrm{kJ/\ mole}}{RT} \right) \exp\left(\frac{W_{\mathrm{int}}}{RT} \right), \tag{8}$$

and when elastoplastic effects are accounted for it becomes

$$c_s^{\sigma} = 3.74 \exp\left(\frac{-12.6\,\text{kJ/ mole}}{RT}\right) \exp\left(\frac{\Delta G_{\alpha-\beta}^{\text{mech}}}{RT}\right). \tag{9}$$

With the solvus concentration known it was possible to calculate the hydride field by coupling the stress enhanced hydrogen diffusion with the material elastoplastic deformation at a crack tip. The hydrogen distribution was calculated by a full transient finite element analysis at each instant of time and the concentration was compared point-wise with the terminal solubility. Hydrides were formed if the point-wise concentration exceeded the terminal solubility in accordance with the Lever rule. The formation of the hydride of course alters the local stress field and requires recalculation of the hydrogen distribution and the terminal solubility. The present calculation is essentially a probabilistic one and does not address the issues associated

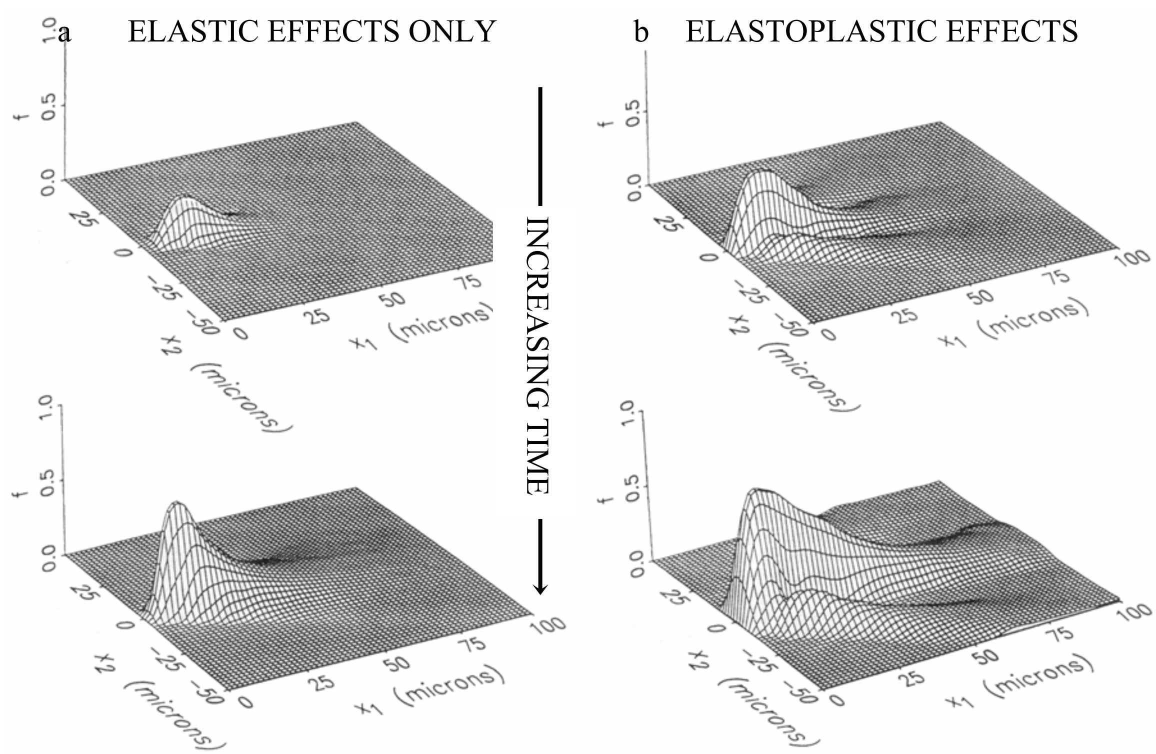

Figure 2: Comparison between purely elastic and elastoplastic accommodation of hydride formation ahead of a crack in niobium.

with hydride shape or the kinetics of the formation of an actual hydride particle. This yields a point density of the hydride termed the "local hydride volume fraction", i.e. the probability of finding a hydride particle at a given location. The results of these calculations with and without plasticity included are compared in Fig 2. Clearly, without the inclusion of plasticity effects the extensive hydride field that is observed experimentally, Fig 1(d), is not obtained.

Hydrogen Effect on Plastic Shear Localization

The shear localization due to solute hydrogen is well documented experimentally but a theoretical explanation is lacking (7). In the hydrogen-containing alloy, localized slip produced steps as large as 1 μm and these resulted in shear band failure. In contrast there was no localization of slip in the uncharged material. In this section a solid mechanics approach to shear localization in the presence of hydrogen is summarized. The approach is based on the analysis proposed by Rice and Rudnicki (17, 18) that localization of deformation into shear bands occurs due to an instability in the rate of equilibrium governing equations for the homogeneous deformation of a material. Rudnicki and Rice (18) have shown that shear banding (or bifurcation of the solution) occurs when the tangent plastic modulus $h = d\sigma / d\varepsilon^p$ (which is always positive for work-hardening materials and continuously decreases with accumulating effective plastic strain ε^p) becomes equal to a critical hardening modulus h_{cr}, which depends on material parameters and the level of stress. The critical hardening modulus is defined by

$$\begin{aligned} \frac{h_{cr}}{G} &= \frac{1+\nu}{9(1-\nu)}(\beta-\mu)^2 - \frac{1+\nu}{2}\left(N_{II} + \frac{\beta+\mu}{3}\right)^2 \\ &+ \frac{\left(4-3N_{II}^2\right)(1+\nu)}{24\sqrt{3}\,(1-\nu)}(\beta-\mu)(\sin 2\theta_0)^2 \frac{\sigma_e}{G} + O\left(\frac{\sigma_e}{G}\right)^2, \end{aligned} \tag{10}$$

where ν is Poisson's ratio, G the shear modulus, $\tan\theta_0 = \sqrt{(\xi - N_{III})/(N_I - \xi)}$, $N_i = \sqrt{3}\sigma_i'/\sigma_e$, $i = I, II, III$ denotes the three principal stress directions, σ_i' the principal deviatoric stress, σ_e the von Mises effective stress, $\xi = \left[(1+\nu)(\beta+\mu)/3\right] - N_{II}(1-\nu)$, β the plastic dilatancy factor, μ the pressure sensitivity of yield, and the loading is such that $N_{III} < \xi < N_I$.

In the absence of hydrogen and in the case of plane strain deformation, the critical modulus h_{cr} is less than zero, and therefore the condition for the bifurcation instability $h = h_{cr}$ is not normally satisfied. Sofronis et al. (19) have recently demonstrated that h_{cr} also depends on the hydrogen concentration and applied stress such that it becomes positive at some critical hydrogen concentration. Consequently, if the condition $h = h_{cr}$ is satisfied locally shear banding becomes possible. The hardening modulus is also dependent on the hydrogen concentration, $h = \frac{1}{3}\left(\frac{\partial\sigma_Y}{\partial\varepsilon^p} + \frac{\partial\sigma_Y}{\partial c}\frac{\partial c}{\partial\varepsilon^p}\right)$, where σ_Y is the flow stress and c is the hydrogen concentration measured in atoms of hydrogen per solvent atom. The effect of hydrogen on h is small in comparison to that on h_{cr}.

To calculate the dependence of h_{cr} and h on the hydrogen concentration, the amount of hydrogen in the material strained in plane strain uniaxial tension was calculated by considering the extent of plastic straining (trapped hydrogen) and hydrostatic stress (hydrogen in normal

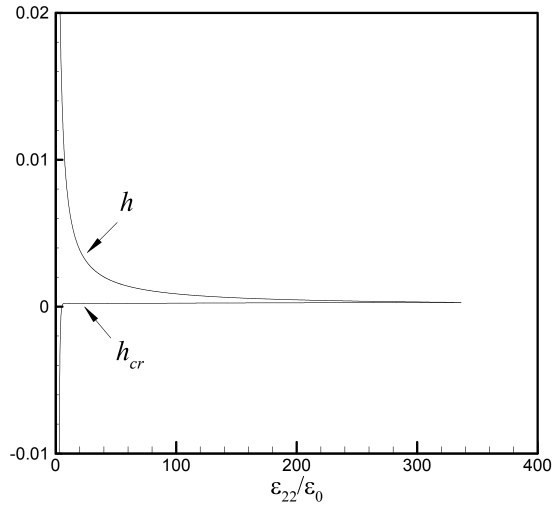

Figure: 3. Dependence of the critical, h_{cr}, and the tangent modulus, h, on the macroscopic strain for an initial hydrogen concentration of H/M = 0.3.

interstitial lattice sites). In view of the very high mobility of solute hydrogen, the hydrogen concentration in trap sites was assumed always to be in equilibrium with hydrogen in interstitial sites, which is also assumed to be in equilibrium with local hydrostatic stress. The calculated hydrogen concentration was then used to estimate the amount of material softening as reflected in the corresponding local flow stress curves (8, 20-24). Figure 3 shows the result of these calculations for h and h_{cr} versus macroscopic strain for a bulk initial hydrogen concentration of c_o= 0.3 in the absence of stress. The critical hardening modulus increases rapidly with strain and assumes a positive value. The point where the two curves intersect indicates the level of the applied load at which shear banding occurs.

Figure 4 shows the normalized true (logarithmic) strain at localization plotted against the initial hydrogen concentration for work hardening exponents n = 5 and n = 10. At hydrogen concentrations $c_o < 0.29$, the softer material n = 10 requires a higher strain to achieve the stress triaxiality to produce the hydrogen concentration needed to cause localization. At hydrogen concentrations above 0.29 material softening dominates and the high stress triaxiality is not so important in satisfying the condition that $h = h_{cr}$. Thus, the present model simulations, which are based on experimentally verified effects, softening and lattice dilatation, predict that hydrogen induced localization of plastic deformation in the form of bands of intense shear is a possible deformation mechanism at the macroscale. The numerical results overestimate the macroscopic strain required for localization as predicted by experiments. It is, however, well known that the von Mises flow theory dramatically overestimates the bifurcation strain. Furthermore, the calculated hydrogen effect can be intensified quantitatively by considering more effective trapping modes of hydrogen such as in the form of atmospheres in the presence of higher stress triaxialities such as those ahead of a crack tip.

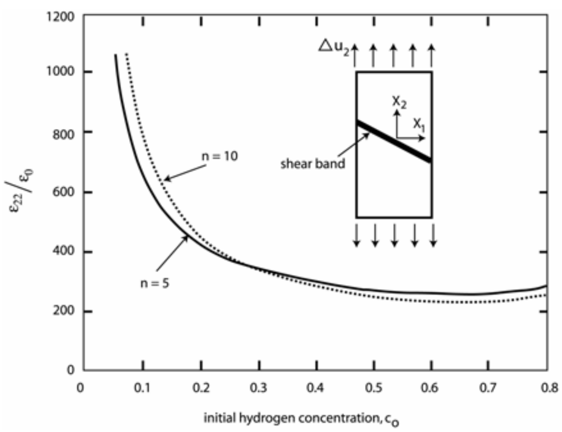

Figure 4: Normalized macroscopic strain at localization as a function of the initial hydrogen concentration, c_o.

Hydrogen–Induced Decohesion

Of all the proposed hydrogen embrittlement mechanisms, decohesion is the one most often cited as the cause of hydrogen-induced failure. In its simplest form this model asserts that hydrogen lowers the cohesive strength of the solid and, consequently, materials fail at lower applied stresses. There are, however, no direct measurements of such an effect and the experimental support is circumstantial. Our lack of knowledge of the dependence of the cohesive strength on the hydrogen concentration illustrates a key issue in that the minimum concentration needed to have a marked effect on the mechanical properties is unknown. In this section, the results of experiments designed to test the possible embrittlement mechanisms in the beta-Ti alloy Timetal® 21S are summarized (25).

This alloy when heat-treated to produce a single-phase microstructure exhibits about 27% ductility when tested in air at room temperature. This ductility is maintained even with a hydrogen concentration of H/M =0.21 (17.7 at % H). At concentrations higher than 0.21, the ductility is reduced to zero and the fracture mode changes from one of ductile microvoid coalescence to transgranular cleavage failure, Fig 5. The cleavage facets show evidence of plasticity in the form of tear ridges, small dimples and a high density of dislocations vicinal to the fracture surface, see for example Fig 5f and 5g. Mechanical property tests showed that there was no measurable effect of hydrogen on Young's modulus, and that the 0.2% offset yield strength decreased with increasing hydrogen content. The crack initiation load (a measure of the fracture toughness) was measured at 248 K and it decreased with increasing hydrogen concentration up to H/M = 0.28 and then remained constant as the hydrogen content was increased further. Limited tests at 298K showed the same trend as at 248 K.

The loss of ductility for a small increase above a critical level might suggest that stress-induced hydride formation and cleavage was occurring. However, the beta phase lattice parameter increases linearly with increasing hydrogen content over the entire hydrogen concentration range studied, which is not consistent with the formation of hydrides. In addition x-ray diffraction and transmission electron microscopy failed to detect any hydrides on or near the fracture surface of the brittle specimens. To test the possibility that the hydrides nucleated in the stress field of the crack and then returned to solid solution following passage of the crack and relief of the stress concentration, electron transparent samples were deformed in a gaseous hydrogen environment in a controlled environment transmission electron microscope. Similar experiments in alpha-Ti produced an extensive hydride field that continued to expand as long as there was a supply of hydrogen, see Fig. 1. The cracked beta-Ti sample was exposed to 70 torr of hydrogen gas at room temperature for 7 days but no hydride field developed. Thus, the stress-induced hydride formation and cleavage mechanism is not responsible for the sharp drop in ductility at H/M > 0.21.

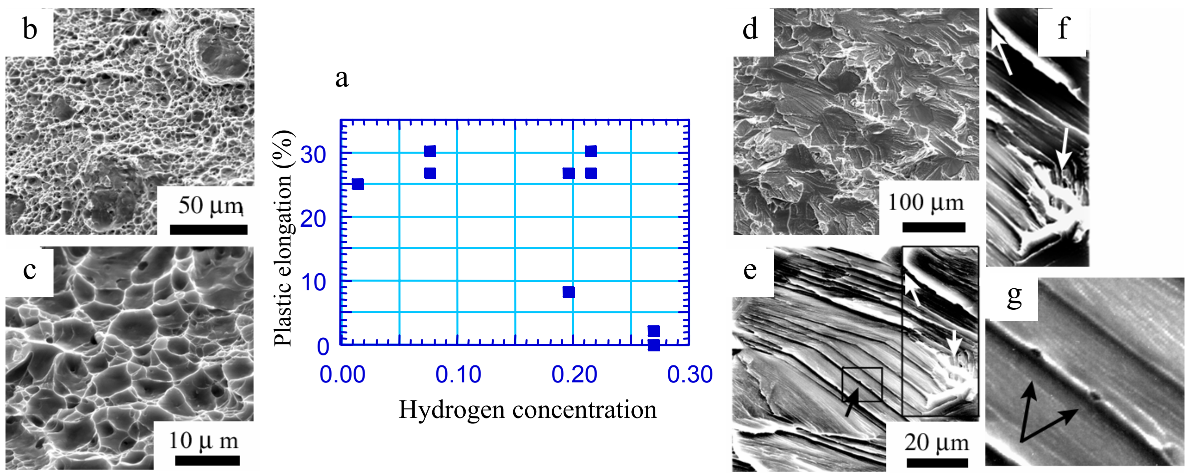

Figure 5: Plastic elongation as a function of hydrogen concentration in Timetal® 21S (a) Fracture surfaces of ductile specimen (b and c). Fracture surface of brittle specimen (d – g)

During the in-situ controlled environment TEM experiments it was observed that hydrogen enhanced the velocity of dislocations in both ductile and brittle samples. Although the hydrogen enhanced localized plasticity mechanism operates in Timetal® 21S it cannot account for the abrupt ductility loss as the enhancement will increase with hydrogen concentration and the effect is observed in both ductile and brittle materials. The last viable mechanism that can account for all of the experimental observations is the decohesion mechanism. As in all other experiments the evidence is circumstantial and is arrived at after the other viable mechanisms have been experimentally tested and discounted. A critical issue is the hydrogen concentration needed to cause a significant reduction in the fracture energy. Unlike in many previous studies the hydrogen concentration at which embrittlement occurs in Timetal® 21S is large. A crude estimate of the decrease in the fracture energy can be obtained from the heats of solutions and absorption and the critical hydrogen concentration at the transition. No stress enhancement of the hydrogen concentration is considered, as the crack propagation rate was fast, 10 mm in less than one second. Unfortunately, the thermodynamic properties of this alloy are not available in the literature, but assuming, for the purpose of discussion, that the values are similar to those in titanium (ΔH_{ads} and ΔH_{soln} are –169 kJ mol^{-1} H_2 and –113.3 kJ mol^{-1} H_2, respectively), and that cleavage occurs on a {110}-type plane, the decrease in fracture energy is approximately 8% of the surface energy of Ti. This is a relatively small change in fracture energy even for such a high hydrogen concentration. Following the argument of Jokl et al. (26) in which the local critical stress intensity factor depends on the cohesive energy as shown schematically in Fig. 6 and assuming that the cohesive energy can be changed by impurities, then solute hydrogen can cause embrittlement provided it reduces the cohesive energy below γ_{cr}. It should be noted that a reduction in cohesive energy also reduces the local critical stress intensity at which the transition occurs and this would necessarily be accompanied by a decrease in plasticity, as it is the same stress field that is responsible for both processes. It is this combined effect that explains the sharp loss of ductility and the reduction in the localized plasticity.

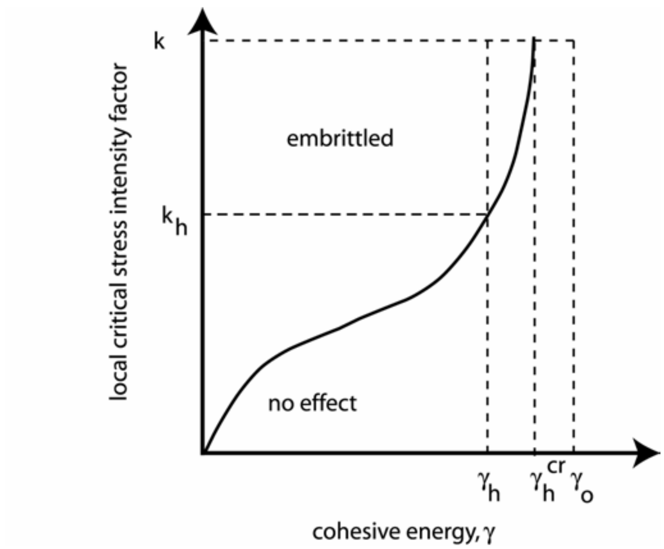

Figure 6: Localized critical stress intensity as a function of cohesive energy.

Conclusion

It has been shown that to simulate the distribution of hydrides ahead of a stress concentration it is necessary, as is observed experimentally, to consider both elastic and plastic mechanisms for accommodating the volume expansion associated with the forming hydride. Analytical calculations have been performed to substantiate the experimental observation that shear localization occurs during deformation in the presence of hydrogen. The shear localization arises from the effect of hydrogen on the tangent and critical moduli, which govern the bifurcation condition. Lastly, we have shown experimentally that decohesion is responsible for the loss of ductility observed in Timatel® 21S, a beta titanium alloy.

Acknowledgements

This manuscript summarizes the cumulative efforts of a number of graduate students and post-doctoral fellows that we have had the pleasure to work with over the years. Their contributions were invaluable. This work was supported by the Department of Energy under grant DEFGO2-96ER45439 and by NASA through grant NAG 8-1751. Use of the microscope facilities at the Center for Microanalysis in the Frederick Seitz Materials Research Laboratory is acknowledged

References

1. I. M. Robertson, "The effect of hydrogen on dislocation dynamics," Engineering Fracture Mechanics, 64 (5) (1999), 649-673.
2. H. K. Birnbaum, et al., "Mechanisms of Hydrogen Related Fracture-A Review," in *Corrosion Deformation Interactions CDI'96*, T. Magnin, Editor. 1997, The Institute of Materials, Great Britain.: Nice, France. p. 172-195.
3. H. K. Birnbaum and P. Sofronis, "Hydrogen-enhanced localized plasticity-a mechanism for hydrogen-related fracture," Mat.Sc. and Eng., A176 (1994), 191-202.
4. C. Hwang and I. M. Bernstein, "Shear Localization in steels (madeup)," Scripta Metall., 16 (1982), 341.
5. J. K. Lin and R. A. Oriani, "The effect of hydrogen on the initiation of shear localization in plain-carbon steels," Acta Metall., 31 (7) (1983), 1071-1077.
6. H. E. Deve, R. J. Asaro, and N. R. Moody, "The influence of hydrogen on the development of localized plastic deformation in internally nitrided single crystals of iron," Scr. Metall., 23 (3) (1989), 389-395.
7. D. G. Ulmer and C. J. Altstetter, "Hydrogen-induced strain localization and failure of austenitic stainless steels at high hydrogen concentrations," Acta Met. et Mat., 39 (6) (1991), 1237-1248.
8. H. K. Birnbaum, "Hydrogen effects on deformation-relation between dislocation behavior and the macroscopic stress-strain behavior," Scr. Metall. Mater., 31 (2) (1994), 149-153.
9. D. P. Abraham and C. J. Altstetter, "Hydrogen-enhanced localization of plasticity in an austenitic stainless steel," Metall. Trans., 26A (1995), 2859-2871.
10. S. P. Lynch, "Mechanisms of hydrogen-assisted cracking," Met. Forum, 2 (3) (1979), 189-200.
11. S. P. Lynch, "Environmentally assisted cracking: an overview of evidence for an absorption-induced localised slip process," Acta Metall., 36 (1988), 2639 - 2661.
12. D. G. Westlake, "A generalized model for hydrogen embrittlement," Trans. ASM, 62 (1969), 1000.
13. H. K. Birnbaum, "Mechanical properties of metal hydrides," J. Less-Common Met., 104 (1) (1984), 31 - 41.
14. D. S. Shih, I. M. Robertson, and H. K. Birnbaum, "Hydrogen embrittlement of alpha titanium: in situ TEM studies," Acta Metall., 36 (1) (1988), 111-124.
15. I. M. Robertson and D. Teter, "Controlled Environment Transmission Electron Microscopy," Journal Microscopy Research and Technique, 42 (1998), 260 - 269.

16. J. Lufrano, P. Sofronis, and H. K. Birnbaum, "Elastoplastically accommodated hydride formation and embrittlement," Journal of the Mechanics & Physics of Solids, 46 (9) (1998), 1497-1520.
17. J. R. Rice, "The localization of plastic deformation," in *Proc. of the 14th Int. Congress on Theoretical and Applied Mechanics*, W.T. Koiter., Editor. 1976, North-Holland Publishing Co: Delft North-Holland. p. 207-220.
18. J. W. Rudnicki and J. R. Rice, "Conditions for the localization of deformation in pressure-sensitive dilatant materials," J. Mech. Phys. Solids, 23 (371-394) (1975).
19. P. Sofronis, Y. M. Liang, and N. Aravas, "Hydrogen induced shear localization of the plastic flow in metals and alloys," European Journal of Mechanics/A Solids, submitted (2001).
20. H. Matsui, H. Kimura, and A. Kimura, "The effect of hydrogen on the mechanical properties of high purity iron. III. The dependence of softening on specimen size and charging current density," Mater. Sci. & Eng., 40 (2) (1979), 227-234.
21. H. Matsui, H. Kimura, and S. Moriya, "The effect of hydrogen on the mechanical properties of high purity iron. I. Softening and hardening of high purity iron by hydrogen charging tensile deformation," Mater. Sci. & Eng., 40 (2) (1979), 207-216.
22. O. A. Onyewuenyi and J. P. Hirth, "The effect of hydrogen on microhardness of spheroidized AISI 1090 steel," Scripta Metall., 15 (1) (1981), 113-118.
23. A. Kimura and H. Kimura, "Hydrogen embrittlement in high purity iron single crystals," Mater. Sci. & Eng., 77 (1986), 75-83.
24. H. Kimura and H. Matsui, "Mechanisms of hydrogen-induced softening and hardening in iron," Scripta Metall., 21 (1987), 319 - 324.
25. D. F. Teter, I. M. Robertson, and H. K. Birnbaum, "The Effects of Hydrogen on The Deformation and Fracture of Beta-Titanium," Acta Mat., Submitted for publication (2001).
26. M. L. Jokl, et al., "On the micromechanics of brittle fracture: existing vs injected cracks," Acta Metall., 37 (1) (1989), 87-97.

List of Recent TAM Reports

No.	*Authors*	*Title*	*Date*
895	Buckmaster, J. D., and M. Short	Cellular instabilities, sub-limit structures, and edge-flames in premixed counterflows—*Combustion Theory and Modeling* **3**, 199–214 (1999)	Oct. 1998
896	Harris, J. G.	*Elastic waves*—Part of a book to be published by Cambridge University Press	Dec. 1998
897	Paris, A. J., and G. A. Costello	Cord composite cylindrical shells—*Journal of Applied Mechanics* **67**, 117–127 (2000)	Dec. 1998
898	Students in TAM 293–294	Thirty-fourth student symposium on engineering mechanics (May 1997), J. W. Phillips, coordinator: Selected senior projects by M. R. Bracki, A. K. Davis, J. A. (Myers) Hommema, and P. D. Pattillo	Dec. 1998
899	Taha, A., and P. Sofronis	A micromechanics approach to the study of hydrogen transport and embrittlement—*Engineering Fracture Mechanics* **68**, 803–837 (2001)	Jan. 1999
900	Ferney, B. D., and K. J. Hsia	The influence of multiple slip systems on the brittle–ductile transition in silicon—*Materials Science Engineering A* **272**, 422–430 (1999)	Feb. 1999
901	Fried, E., and A. Q. Shen	Supplemental relations at a phase interface across which the velocity and temperature jump—*Continuum Mechanics and Thermodynamics* **11**, 277–296 (1999)	Mar. 1999
902	Paris, A. J., and G. A. Costello	Cord composite cylindrical shells: Multiple layers of cords at various angles to the shell axis	Apr. 1999
903	Ferney, B. D., M. R. DeVary, K. J. Hsia, and A. Needleman	Oscillatory crack growth in glass—*Scripta Materialia* **41**, 275–281 (1999)	Apr. 1999
904	Fried, E., and S. Sellers	Microforces and the theory of solute transport—*Zeitschrift für angewandte Mathematik und Physik* **51**, 732–751 (2000)	Apr. 1999
905	Balachandar, S., J. D. Buckmaster, and M. Short	The generation of axial vorticity in solid-propellant rocket-motor flows—*Journal of Fluid Mechanics* (submitted)	May 1999
906	Aref, H., and D. L. Vainchtein	The equation of state of a foam—*Physics of Fluids* **12**, 23–28 (2000)	May 1999
907	Subramanian, S. J., and P. Sofronis	Modeling of the interaction between densification mechanisms in powder compaction—*International Journal of Solids and Structures*, in press (2000)	May 1999
908	Aref, H., and M. A. Stremler	Four-vortex motion with zero total circulation and impulse—*Physics of Fluids* **11,** 3704-3715	May 1999
909	Adrian, R. J., K. T. Christensen, and Z.-C. Liu	On the analysis and interpretation of turbulent velocity fields—*Experiments in Fluids* **29**, 275–290 (2000)	May 1999
910	Fried, E., and S. Sellers	Theory for atomic diffusion on fixed and deformable crystal lattices—*Journal of Elasticity* **59**, 67–81 (2000)	June 1999
911	Sofronis, P., and N. Aravas	Hydrogen induced shear localization of the plastic flow in metals and alloys—*European Journal of Mechanics/A Solids* (submitted)	June 1999
912	Anderson, D. R., D. E. Carlson, and E. Fried	A continuum-mechanical theory for nematic elastomers—*Journal of Elasticity* **56**, 33–58 (1999)	June 1999
913	Riahi, D. N.	High Rayleigh number convection in a rotating melt during alloy solidification—*Recent Developments in Crystal Growth Research* **2**, 211–222 (2000)	July 1999
914	Riahi, D. N.	Buoyancy driven flow in a rotating low Prandtl number melt during alloy solidification—*Current Topics in Crystal Growth Research* **5**, 151–161 (2000)	July 1999
915	Adrian, R. J.	On the physical space equation for large-eddy simulation of inhomogeneous turbulence—*Physics of Fluids* (submitted)	July 1999

No.	Authors	Title	Date
916	Riahi, D. N.	Wave and vortex generation and interaction in turbulent channel flow between wavy boundaries—*Journal of Mathematical Fluid Mechanics* (submitted)	July 1999
917	Boyland, P. L., M. A. Stremler, and H. Aref	Topological fluid mechanics of point vortex motions	July 1999
918	Riahi, D. N.	Effects of a vertical magnetic field on chimney convection in a mushy layer—*Journal of Crystal Growth* **216**, 501–511 (2000)	Aug. 1999
919	Riahi, D. N.	Boundary mode–vortex interaction in turbulent channel flow over a non-wavy rough wall—*Proceedings of the Royal Society of London A*, in press (2001)	Sept. 1999
920	Block, G. I., J. G. Harris, and T. Hayat	Measurement models for ultrasonic nondestructive evaluation—*IEEE Transactions on Ultrasonics, Ferroelectrics, and Frequency Control* **47**, 604–611 (2000)	Sept. 1999
921	Zhang, S., and K. J. Hsia	Modeling the fracture of a sandwich structure due to cavitation in a ductile adhesive layer—*Journal of Applied Mechanics* (submitted)	Sept. 1999
922	Nimmagadda, P. B. R., and P. Sofronis	Leading order asymptotics at sharp fiber corners in creeping-matrix composite materials	Oct. 1999
923	Yoo, S., and D. N. Riahi	Effects of a moving wavy boundary on channel flow instabilities—*Theoretical and Computational Fluid Dynamics* (submitted)	Nov. 1999
924	Adrian, R. J., C. D. Meinhart, and C. D. Tomkins	Vortex organization in the outer region of the turbulent boundary layer—*Journal of Fluid Mechanics* **422**, 1–53 (2000)	Nov. 1999
925	Riahi, D. N., and A. T. Hsui	Finite amplitude thermal convection with variable gravity—*International Journal of Mathematics and Mathematical Sciences* **25**, 153–165 (2001)	Dec. 1999
926	Kwok, W. Y., R. D. Moser, and J. Jiménez	A critical evaluation of the resolution properties of *B*-spline and compact finite difference methods—*Journal of Computational Physics* (submitted)	Feb. 2000
927	Ferry, J. P., and S. Balachandar	A fast Eulerian method for two-phase flow—*International Journal of Multiphase Flow*, in press (2000)	Feb. 2000
928	Thoroddsen, S. T., and K. Takehara	The coalescence–cascade of a drop—*Physics of Fluids* **12**, 1257–1265 (2000)	Feb. 2000
929	Liu, Z.-C., R. J. Adrian, and T. J. Hanratty	Large-scale modes of turbulent channel flow: Transport and structure—*Journal of Fluid Mechanics* (submitted)	Feb. 2000
930	Borodai, S. G., and R. D. Moser	The numerical decomposition of turbulent fluctuations in a compressible boundary layer—*Theoretical and Computational Fluid Dynamics* (submitted)	Mar. 2000
931	Balachandar, S., and F. M. Najjar	Optimal two-dimensional models for wake flows—*Physics of Fluids*, in press (2000)	Mar. 2000
932	Yoon, H. S., K. V. Sharp, D. F. Hill, R. J. Adrian, S. Balachandar, M. Y. Ha, and K. Kar	Integrated experimental and computational approach to simulation of flow in a stirred tank—*Chemical Engineering Sciences* (submitted)	Mar. 2000
933	Sakakibara, J., Hishida, K., and W. R. C. Phillips	On the vortical structure in a plane impinging jet—*Journal of Fluid Mechanics* **434**, 273–300 (2001)	Apr. 2000
934	Phillips, W. R. C.	Eulerian space–time correlations in turbulent shear flows	Apr. 2000
935	Hsui, A. T., and D. N. Riahi	Onset of thermal–chemical convection with crystallization within a binary fluid and its geological implications—*Geochemistry, Geophysics, Geosystems* **2**, 2000GC000075 (2001)	Apr. 2000
936	Cermelli, P., E. Fried, and S. Sellers	Configurational stress, yield, and flow in rate-independent plasticity—*Proceedings of the Royal Society of London A* **457**, 1447–1467 (2001)	Apr. 2000

List of Recent TAM Reports (cont'd)

No.	*Authors*	*Title*	*Date*
937	Adrian, R. J., C. Meneveau, R. D. Moser, and J. J. Riley	Final report on 'Turbulence Measurements for Large-Eddy Simulation' workshop	Apr. 2000
938	Bagchi, P., and S. Balachandar	Linearly varying ambient flow past a sphere at finite Reynolds number—Part 1: Wake structure and forces in steady straining flow	Apr. 2000
939	Gioia, G., A. DeSimone, M. Ortiz, and A. M. Cuitiño	Folding energetics in thin-film diaphragms	Apr. 2000
940	Chaïeb, S., and G. H. McKinley	Mixing immiscible fluids: Drainage induced cusp formation	May 2000
941	Thoroddsen, S. T., and A. Q. Shen	Granular jets—*Physics of Fluids* **13**, 4–6 (2001)	May 2000
942	Riahi, D. N.	Non-axisymmetric chimney convection in a mushy layer under a high-gravity environment—In *Centrifugal Materials Processing* (L. L. Regel and W. R. Wilcox, eds.), 295–302 (2001)	May 2000
943	Christensen, K. T., S. M. Soloff, and R. J. Adrian	PIV Sleuth: Integrated particle image velocimetry interrogation/validation software	May 2000
944	Wang, J., N. R. Sottos, and R. L. Weaver	Laser induced thin film spallation—*Experimental Mechanics* (submitted)	May 2000
945	Riahi, D. N.	Magnetohydrodynamic effects in high gravity convection during alloy solidification—In *Centrifugal Materials Processing* (L. L. Regel and W. R. Wilcox, eds.), 317–324 (2001)	June 2000
946	Gioia, G., Y. Wang, and A. M. Cuitiño	The energetics of heterogeneous deformation in open-cell solid foams	June 2000
947	Kessler, M. R., and S. R. White	Self-activated healing of delamination damage in woven composites—*Composites A: Applied Science and Manufacturing* **32**, 683–699 (2001)	June 2000
948	Phillips, W. R. C.	On the pseudomomentum and generalized Stokes drift in a spectrum of rotational waves—*Journal of Fluid Mechanics* **430**, 209–229 (2001)	July 2000
949	Hsui, A. T., and D. N. Riahi	Does the Earth's nonuniform gravitational field affect its mantle convection?—*Physics of the Earth and Planetary Interiors* (submitted)	July 2000
950	Phillips, J. W.	Abstract Book, 20th International Congress of Theoretical and Applied Mechanics (27 August – 2 September, 2000, Chicago)	July 2000
951	Vainchtein, D. L., and H. Aref	Morphological transition in compressible foam—*Physics of Fluids* **13**, 2152–2160 (2001)	July 2000
952	Chaïeb, S., E. Sato-Matsuo, and T. Tanaka	Shrinking-induced instabilities in gels	July 2000
953	Riahi, D. N., and A. T. Hsui	A theoretical investigation of high Rayleigh number convection in a nonuniform gravitational field—*Acta Mechanica* (submitted)	Aug. 2000
954	Riahi, D. N.	Effects of centrifugal and Coriolis forces on a hydromagnetic chimney convection in a mushy layer—*Journal of Crystal Growth* **226**, 393–405 (2001)	Aug. 2000
955	Fried, E.	An elementary molecular-statistical basis for the Mooney and Rivlin–Saunders theories of rubber-elasticity—*Journal of the Mechanics and Physics of Solids*, in press (2001)	Sept. 2000
956	Phillips, W. R. C.	On an instability to Langmuir circulations and the role of Prandtl and Richardson numbers—*Journal of Fluid Mechanics*, in press (2001)	Sept. 2000
957	Chaïeb, S., and J. Sutin	Growth of myelin figures made of water soluble surfactant—Proceedings of the 1st Annual International IEEE–EMBS Conference on Microtechnologies in Medicine and Biology (October 2000, Lyon, France), 345–348	Oct. 2000

No.	*Authors*	*Title*	*Date*
958	Christensen, K. T., and R. J. Adrian	Statistical evidence of hairpin vortex packets in wall turbulence—*Journal of Fluid Mechanics* **431**, 433–443 (2001)	Oct. 2000
959	Kuznetsov, I. R., and D. S. Stewart	Modeling the thermal expansion boundary layer during the combustion of energetic materials—*Combustion and Flame*, in press (2001)	Oct. 2000
960	Zhang, S., K. J. Hsia, and A. J. Pearlstein	Potential flow model of cavitation-induced interfacial fracture in a confined ductile layer—*Journal of the Mechanics and Physics of Solids* (submitted)	Nov. 2000
961	Sharp, K. V., R. J. Adrian, J. G. Santiago, and J. I. Molho	Liquid flows in microchannels—Chapter 6 of *CRC Handbook of MEMS* (M. Gad-el-Hak, ed.) (2001)	Nov. 2000
962	Harris, J. G.	Rayleigh wave propagation in curved waveguides—*Wave Motion*, in press (2001)	Jan. 2001
963	Dong, F., A. T. Hsui, and D. N. Riahi	A stability analysis and some numerical computations for thermal convection with a variable buoyancy factor—*Geophysical and Astrophysical Fluid Dynamics* (submitted)	Jan. 2001
964	Phillips, W. R. C.	Langmuir circulations beneath growing or decaying surface waves—*Journal of Fluid Mechanics* (submitted)	Jan. 2001
965	Bdzil, J. B., D. S. Stewart, and T. L. Jackson	Program burn algorithms based on detonation shock dynamics—*Journal of Computational Physics* (submitted)	Jan. 2001
966	Bagchi, P., and S. Balachandar	Linearly varying ambient flow past a sphere at finite Reynolds number: Part 2—Equation of motion—*Journal of Fluid Mechanics* (submitted)	Feb. 2001
967	Cermelli, P., and E. Fried	The evolution equation for a disclination in a nematic fluid—*Proceedings of the Royal Society A*, in press (2001)	Apr. 2001
968	Riahi, D. N.	Effects of rotation on convection in a porous layer during alloy solidification—Chapter in *Transport Phenomena in Porous Media* (D. B. Ingham and I. Pop, eds.), Oxford: Elsevier Science (2001)	Apr. 2001
969	Damljanovic, V., and R. L. Weaver	Elastic waves in cylindrical waveguides of arbitrary cross section—*Journal of Sound and Vibration* (submitted)	May 2001
970	Gioia, G., and A. M. Cuitiño	Two-phase densification of cohesive granular aggregates	May 2001
971	Subramanian, S. J., and P. Sofronis	Calculation of a constitutive potential for isostatic powder compaction—*International Journal of Mechanical Sciences* (submitted)	June 2001
972	Sofronis, P., and I. M. Robertson	Atomistic scale experimental observations and micromechanical/continuum models for the effect of hydrogen on the mechanical behavior of metals—*Philosophical Magazine* (submitted)	June 2001
973	Pushkin, D. O., and H. Aref	Self-similarity theory of stationary coagulation—*Physics of Fluids* (submitted)	July 2001
974	Lian, L., and N. R. Sottos	Stress effects in ferroelectric thin films—*Journal of the Mechanics and Physics of Solids* (submitted)	Aug. 2001
975	Fried, E., and R. E. Todres	Prediction of disclinations in nematic elastomers—*Proceedings of the National Academy of Sciences* (submitted)	Aug. 2001
976	Fried, E., and V. A. Korchagin	Striping of nematic elastomers—*International Journal of Solids and Structures* (submitted)	Aug. 2001
977	Riahi, D. N.	On nonlinear convection in mushy layers: Part I. Oscillatory modes of convection—*Journal of Fluid Mechanics* (submitted)	Sept. 2001
978	Sofronis, P., I. M. Robertson, Y. Liang, D. F. Teter, and N. Aravas	Recent advances in the study of hydrogen embrittlement at the University of Illinois—Invited paper, Hydrogen–Corrosion Deformation Interactions (Sept. 16–21, 2001, Jackson Lake Lodge, Wyo.)	Sept. 2001